SUPPORTING INFORMATION

Femtosecond to millisecond studies of electron transfer processes in donor-(π-spacer)-acceptor series of organic dyes for solar cells interacting with titania nanoparticles and ordered nanotube array films

Marcin Ziółek,[a] Boiko Cohen,[a] Xichuan Yang,[b] Licheng Sun, [c] Maggie Paulose,[d] Oomman K. Varghese,[d] Craig A. Grimes,[e] Abderrazzak Douhal [a] *

[a] *Departamento de Química Física, Facultad de Ciencias Ambientales y Bioquimica and Inamol, Universidad de Castilla-La Mancha, Avda. Carlos III, S.N., 45071 Toledo, Spain.*

[b] *State Key Laboratory of Fine Chemicals, Dalian University of Technology, Dalian 116012, China.*

[c] *School of Chemical Science and Engineering, Department of Chemistry, Royal Institute of Technology (KTH), 10044 Stockholm, Sweden.*

[d] *The Materials Research Institute, The Pennsylvania State University, University Park, PA 16802 USA.*

[e] *Photonic Fuels LLC, Naval Ship Yard, Philadelphia, PA 19112 USA*

*corresponding author: abderrazzak.douhal@uclm.es

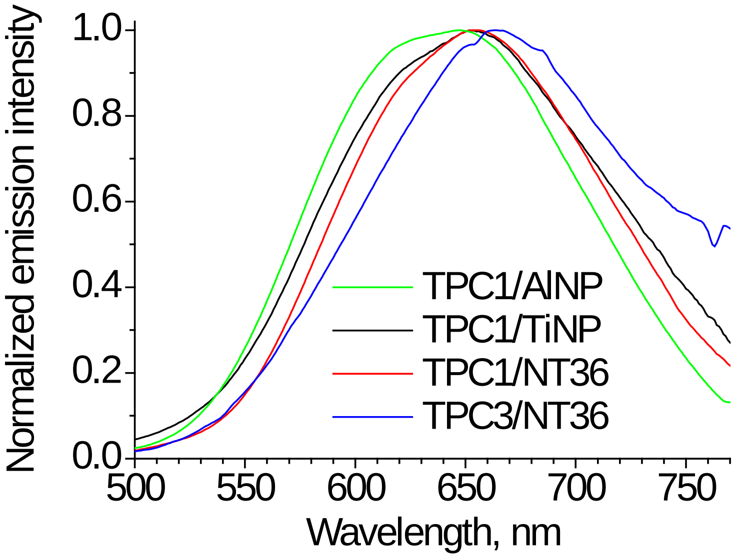

Figure S1. Comparison of stationary emission (excitation 420 nm) spectra of TPC1 and TPC3 on different films.

Table S1.

Comparison of the properties of different solvents and semiconductors used to study the photobehaviour of TPC1 dye.

Material	Dielectric constant	Refractive index	Polarity function $f(\varepsilon,n^2)$ *	Stokes shift for TPC1,cm^{-1}
n-hexane	2	1.43	0.00	2 700
DCM	9	1.42	0.22	8 200
ACN	38	1.35	0.30	10 000
Al_2O_3	10	1.7	0.15	9 400
TiO_2	85	2.5	0.10	9 400

* Lippert-Mataga polarity function $f(\varepsilon,n^2)= [(\varepsilon-1)/(2\varepsilon+1)] - [(n^2-1)/(2n^2+1)]$

.

Table S2.

Comparison of dipole moments and concentration of common polar solvents (DCM and ACN) and TPC1 dye in 700 nm film layer.

	Ground state dipole moment	Concentration
DCM	1.6 D	19 M (in bulk)
ACN	3.9 D	16 M (in bulk)
TPC1 on alumina and titania	10 D	0.2 M (averaged in 700 nm layer)

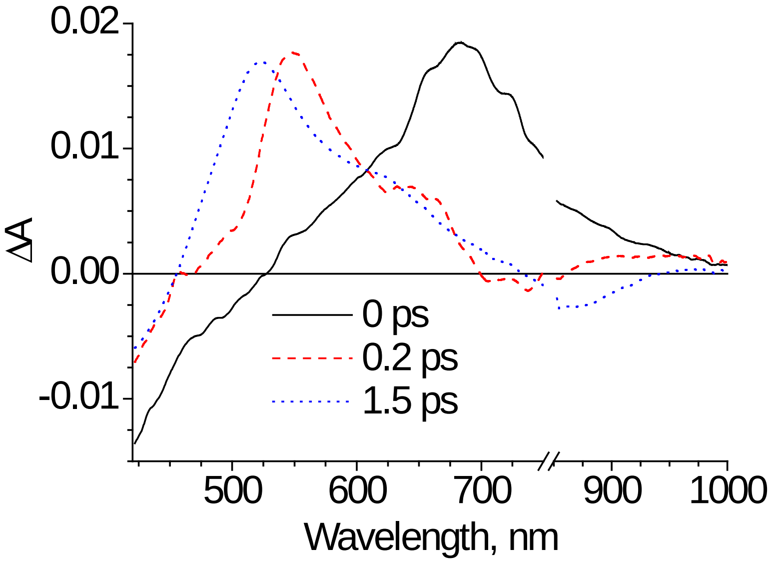

Figure S2. Representative transient absorption spectra of TPC1 (c=0.3 x 10^{-4} M) in ACN solution, at selected delays between pump (400 nm) and probe pulses. The spectra at particular delays correspond to the spectra of: locally excited state (0 ps), charge transfer state before solvation (0.2 ps) and charge transfer state after solvation (1.5 ps).

Table S3.

Values of the time constants (τ_i) and their fractional amplitudes (A_i, a negative value indicates a rise time) obtained from three-exponential functions used to fit the fs absorption transients at the indicated probe wavelengths (λ) of TPC1/NT36. The full width at half maximum (FWHM) of intensity of fitted IRF is 150 fs.

λ /nm	A_1	τ_1 / ps	A_2	τ_2 / ps	A_3	τ_3 / ps
420	-0.0147	1.33	-0.0077	76	-0.0257	1190
450	-0.0083	1.80	-0.0055	86	-0.0310	1180
490	0.0035	1.78	-	-	-0.0168	1390
550	0.0093	1.12	0.0051	38	0.0099	1200
650	0.0126	0.13	0.0083	1.50	0.0045	750
900	0.0029	0.10	0.0015	3.0	0.0012	1500

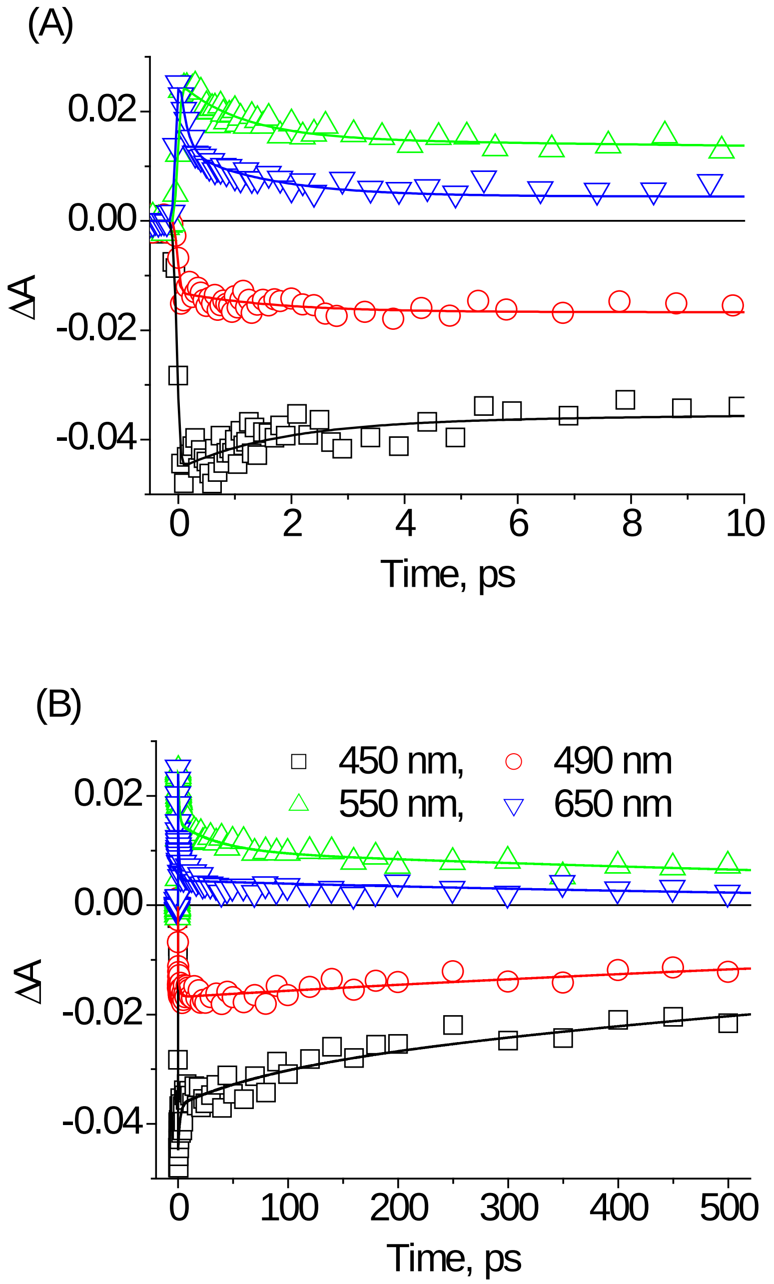

Figure S3. Representative transient absorption kinetics of TPC1/NT36 in shorter (A) and longer (B) time scales, upon excitation at 400 nm and at the indicated probe wavelengths. The solid lines are from the best fit. See Table S3 for the fit parameters. The IRF was 110 fs (FWHM).

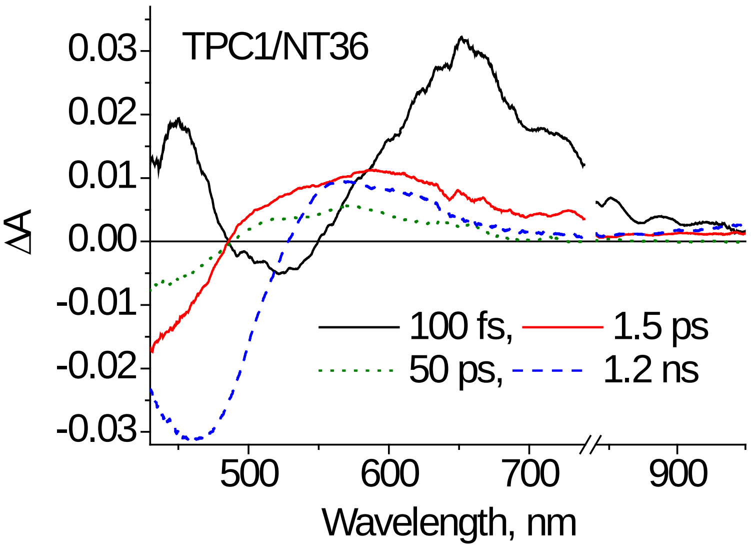

Figure S4. Pre-exponential factor spectra obtained from 4-exponential global analysis of the transient absorption spectra of TPC1/NT36. The negative values indicate a rising component, while the positive values – a decay component. The fitted time components are indicated in the figure. The IRF was 150 fs (FWHM).

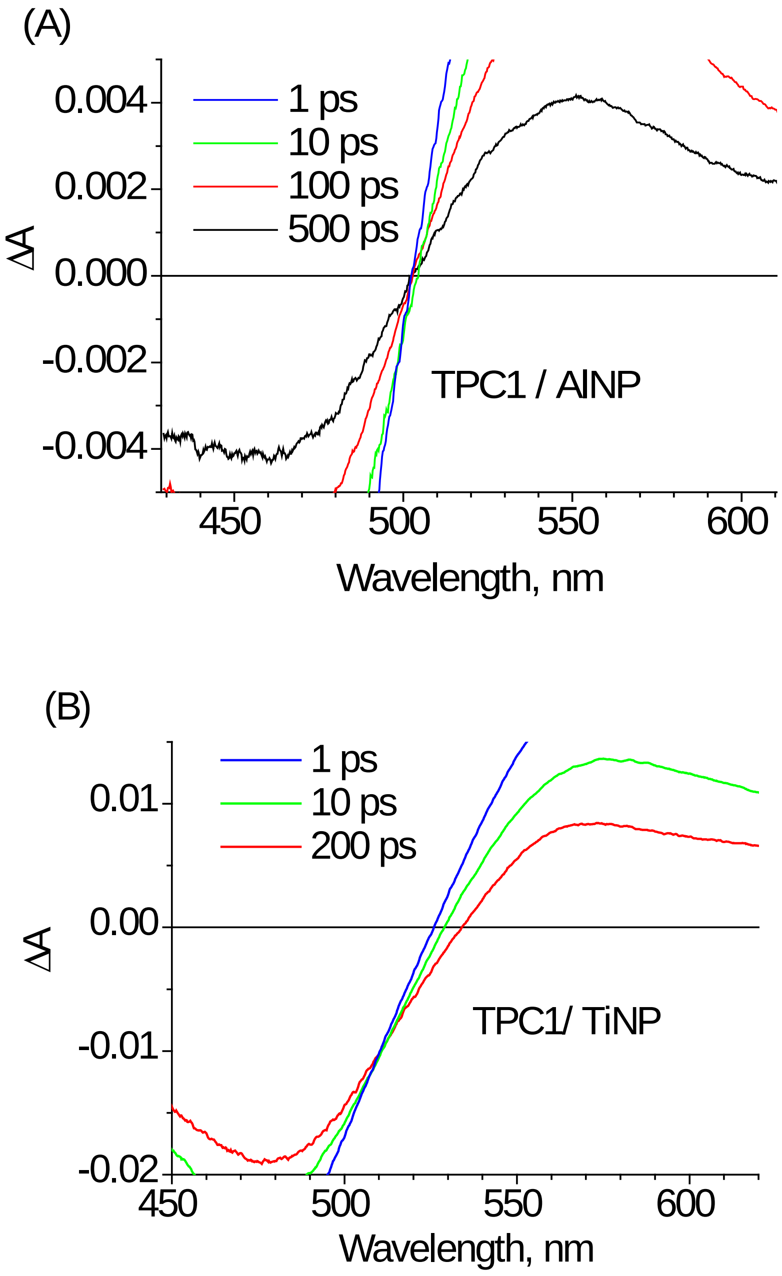

Figure S5. Transient absorption spectra of (A) TPC1/AlNP and (B) TPC1/TiNP at selected delays between pump (400 nm) and probe pulses in the enlarged range of absorption changes, close to ΔA=0.

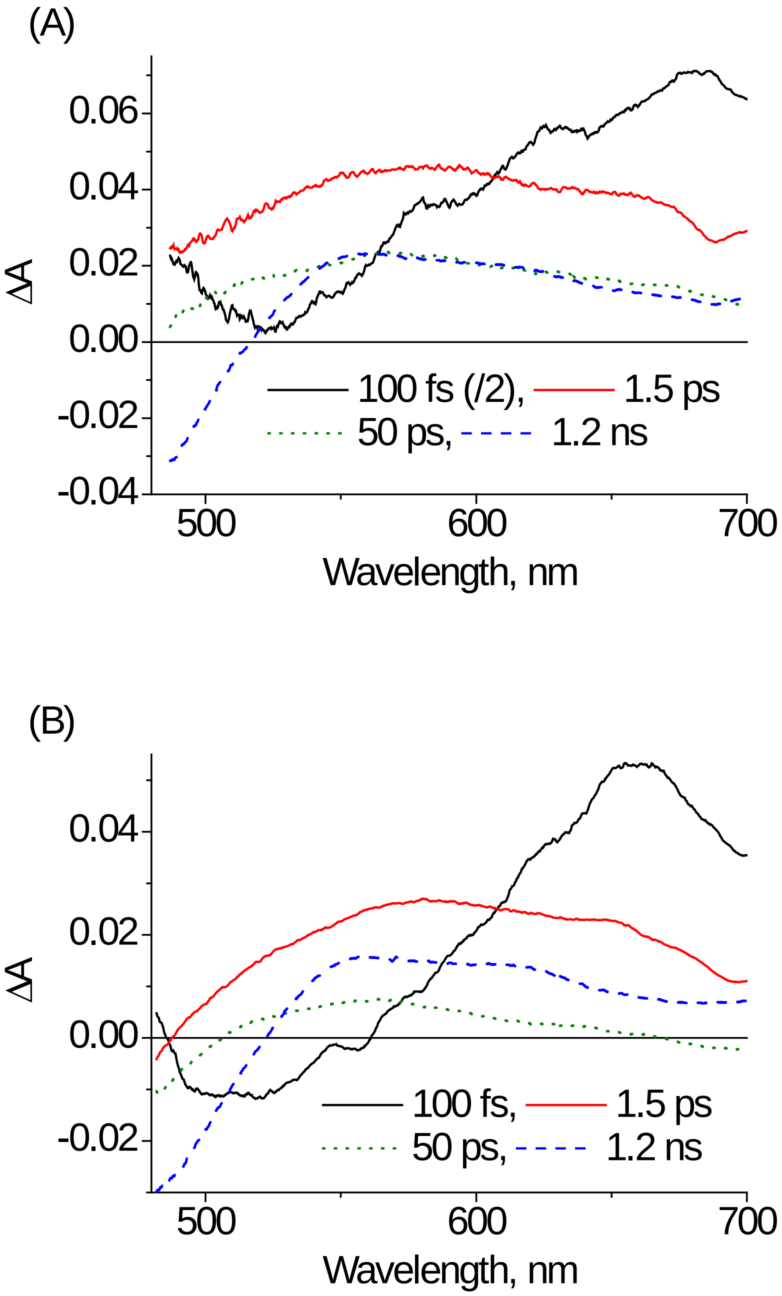

Figure S6. Pre-exponential factor spectra obtained from the global analysis of the transient absorption spectra of (A) TPC1/NT70 and (B) TPC1/NP, both 2 μm thick. The negative values indicate a rising component, while the positive values – a decay component. The time components used to fit the spectra are indicated in the figure. The IRF was 150 fs (FWHM).

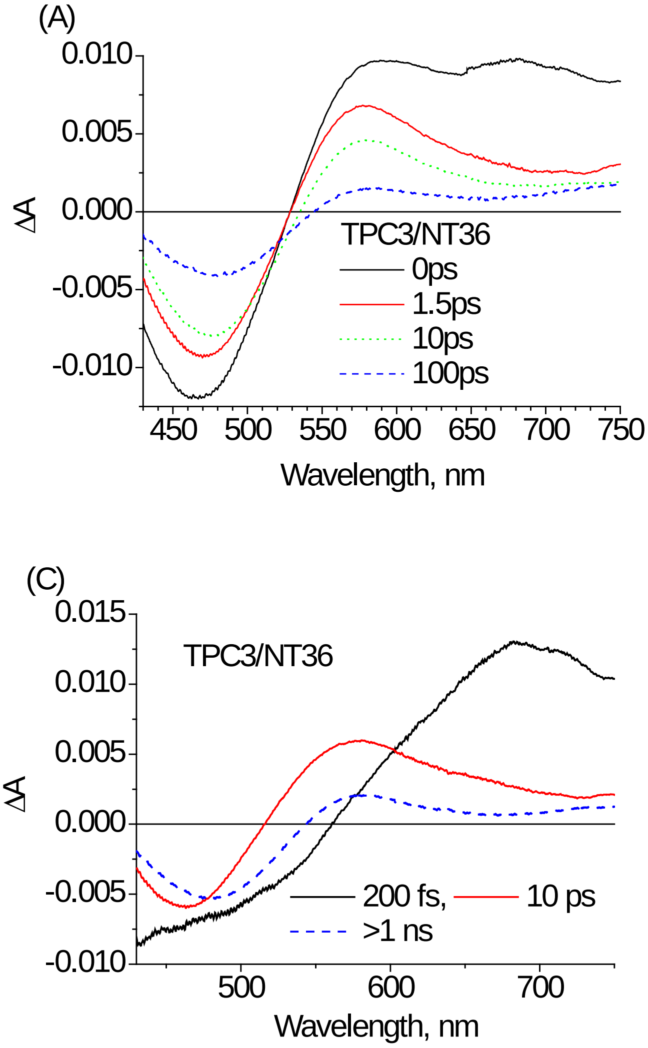

Figure S7. (A) Representative transient absorption spectra (ΔA is the difference between the absorbance of the probe and reference pulse) of TPC3/NT36 at selected delays between pump (400 nm) and probe pulses. (B) Pre-exponential factor spectra obtained from 3-exponential global analysis of the transient absorption spectra of TPC3/NT36. The negative values indicate a rising component, while the positive values – a decay component. The fitted time components are indicated in the figure. The IRF was 150 fs (FWHM).

Table S4.

Values of the time constants (τ_i) and their fractional amplitudes (A_i, normalized to 1) of: (A) TPC1/AlNP, and (B) TPC1/TiNP, at the indicated emission wavelengths and upon excitation at 420 nm sample obtained from two- or three exponential functions, used to fit the fs transient emission (convoluted with an IRF of 180 fs).

(A)

λ /nm	A_1	τ_1 / ps	A_2	τ_2 / ps	A_3	τ_3 / ps
500	0.76	0.16	0.26	1.9	-	-
600	0.39	0.53	0.44	8	0.17	130
680	0.35	1.9	0.40	22	0.26	270

(B)

λ /nm	A_1	τ_1 / ps	A_2	τ_2 / ps	A_3	τ_3 / ps
500	0.78	0.13	0.22	1.1	-	-
600	0.62	0.44	0.31	2.6	0.07	27
680	0.61	0.67	0.30	4.7	0.09	41

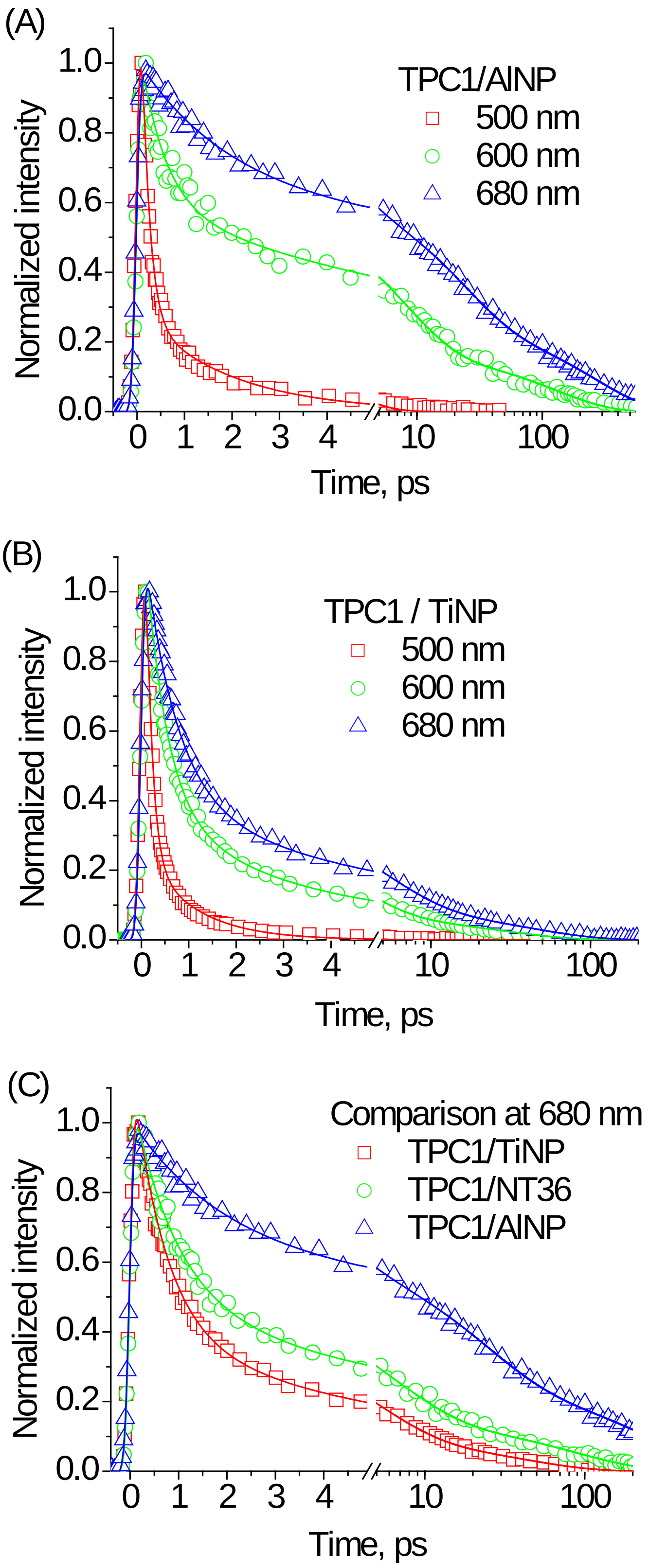

Figure S8. Emission transients of (A) TPC1/AlNP, (B) TPC1/TiNP at the indicated wavelengths of observation, and (C) different samples observed at 680 nm, all upon excitation at 420 nm. The solid lines are from the best fit (see Table S4). A part of the “x” axis corresponding to long times of observation is in a logarithmic scale.

Scheme S1.

Schematic representation of the electron injection model from different vibrational states of TPC1 interacting with titania nanoparticles. The vertical axis represents energy (not in scale), while the horizontal one – the density of acceptor states in the titania conduction band and trap states. The energy shifts of density functions (g_i) are due to the heterogeneity of the sample. The times were taken from the TPC1/TiNP results (Table S3B).

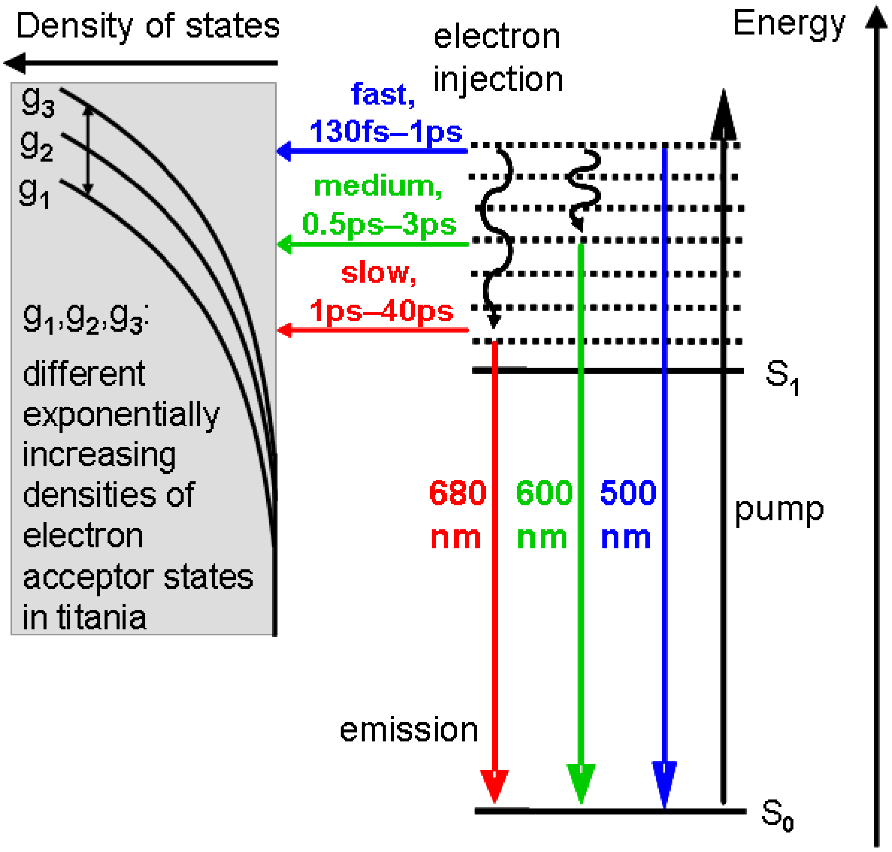

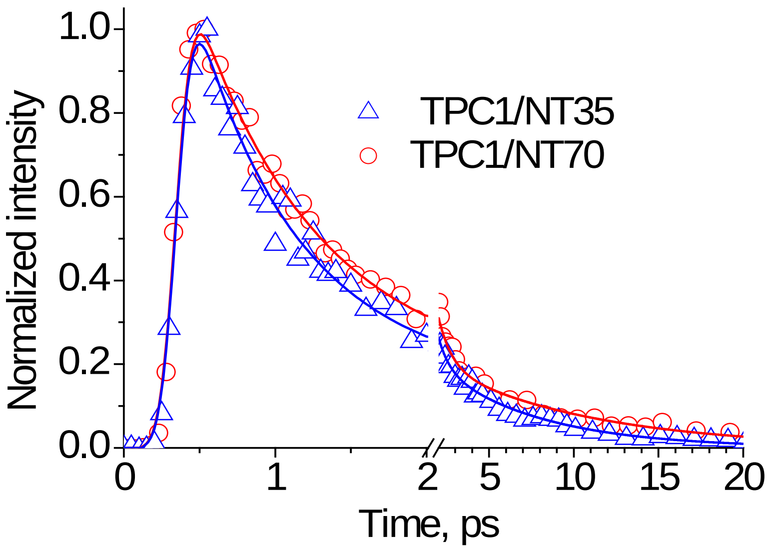

Figure S9. Comparison of the femtosecond emission transients of TPC1 with two different titania nanotubes observed at 600 nm. The solid lines are from the best fit.

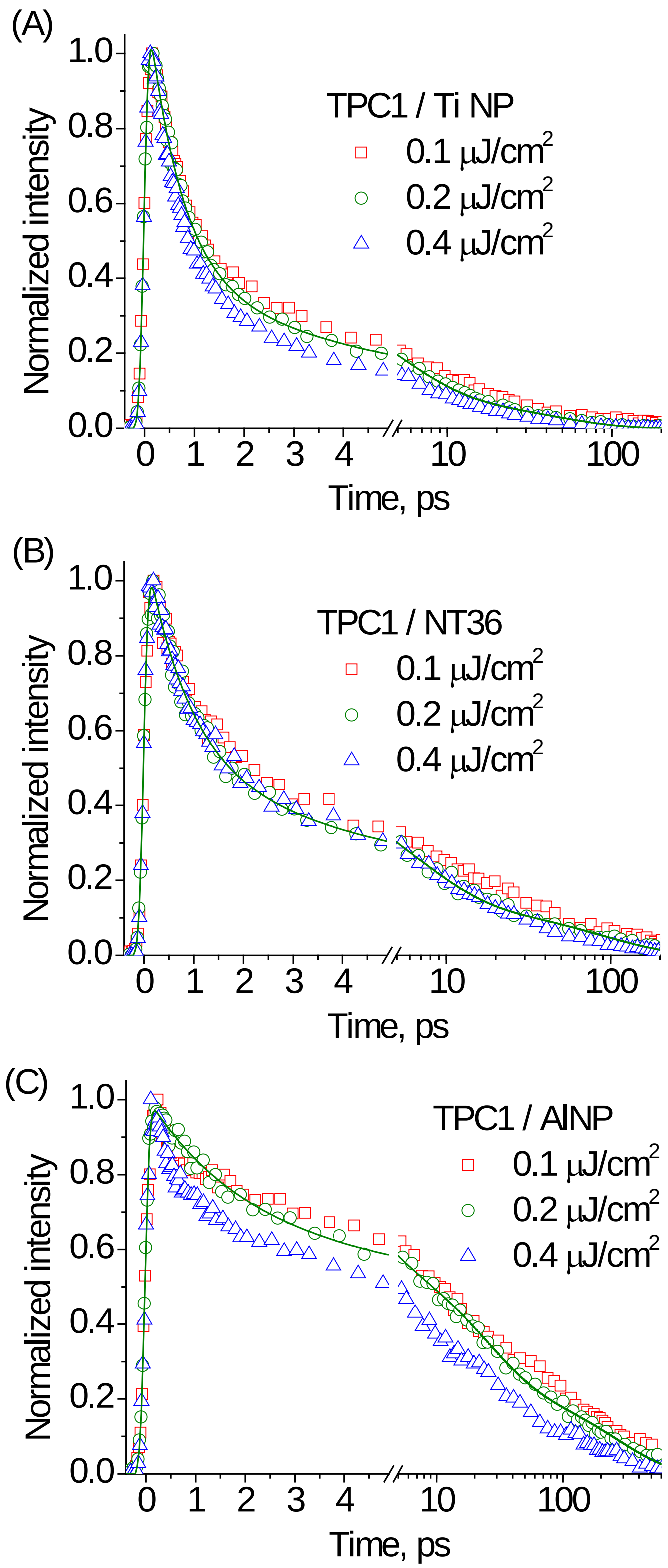

Figure S10. Comparison of the pump pulse energy effect on the emission transients of (A) TPC1/TiNP, (B) TPC1/TiNP and (C) TPC1/AlNP, at 680 nm observation, and upon excitation at 420 nm. The solid lines are from the best fit at 0.2 μJ/cm^2 (see Tables 3 and S4). A part of the "x" axis corresponding to long times of observation is in a logarithmic scale.

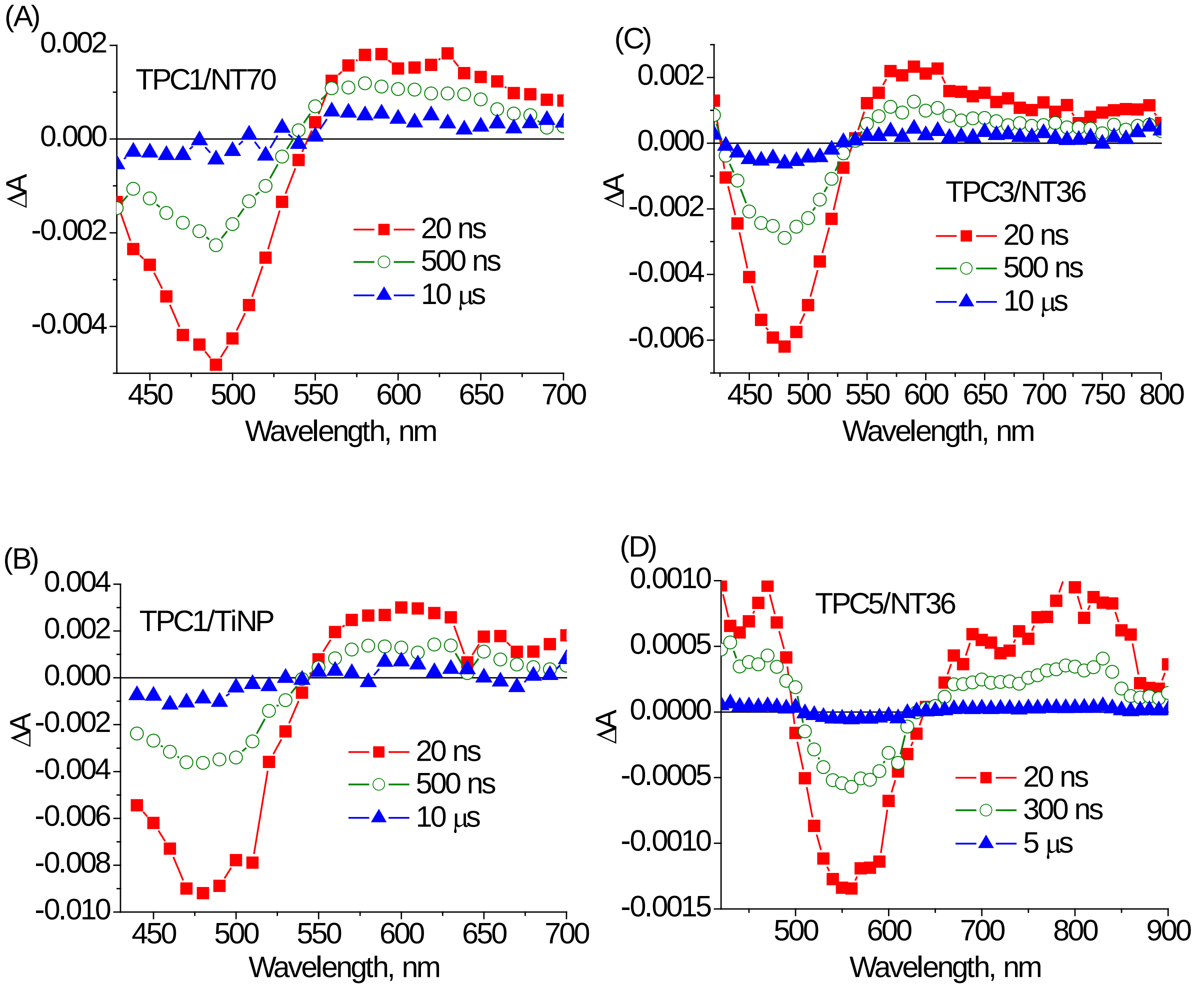

Figure S11. Representative transient absorption spectra of (A) TPC1/NT70, (B) TPC1/TiNP, (C) TPC3/NT36, (D) TPC5/NT36, at selected delays between pump (410 nm, 1 mJ) and probe pulses in flash photolysis experiment.

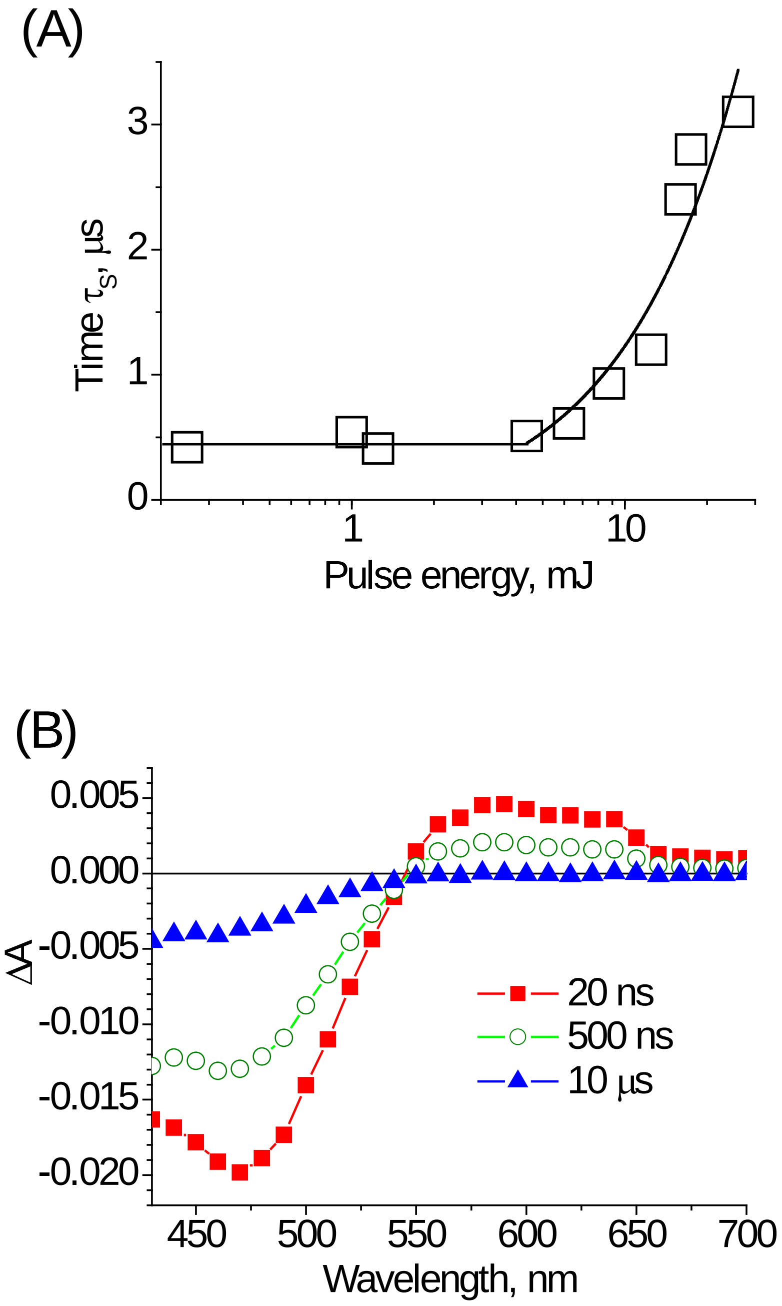

Figure S12. (A) Characteristic time, τ_S, obtained from the best stretched exponential fit (at fixed dispersion parameter $\alpha = 0.33$) of bleach recovery kinetics measured for TPC1/NP at probe wavelength of 480 nm and at different pump pulse energies (the energy axis is in logarithmic scale). The solid line has no mathematical meaning and only shows the observed trend. (B) Transient absorption spectra of TPC1/NP at selected delays between pump and probe pulses for high pump energy (15 mJ).

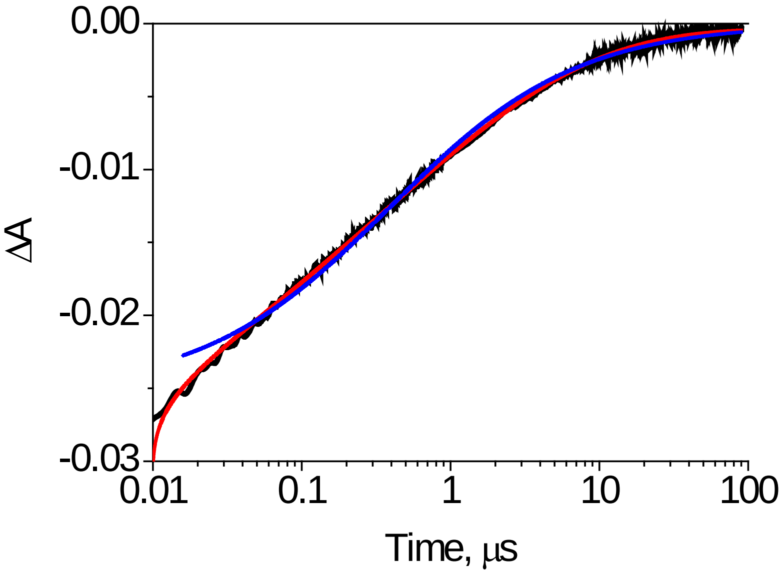

Figure S13. The comparison of stretched exponential fit (red) and the fit of the analytical function for random flight model [1] (blue) to the recombination kinetics of TPC1/NT36 (black) measured at 480 nm upon 410 nm excitation and energy of 1 mJ (density about 2 mJ/cm^2). The analytical function has been taken in the following form: $f(t) = A / (1+B t^m)$, where A is proportional to signal amplitude, B is proportional to the ratio of the number of trap states to the number of injected electrons, and m is the parameter describing exponential distribution of trap states [1]. The fitted parameters are: A=-0.050, B=1.93 and m=0.69. The parameters for the stretched exponential function fit are: τ_S = 0.46 μs and α = 0.33 (see eq. (1)).

1 A. V. Barzykin and M. Tachiya, *J. Phys. Chem. A*, 2002, **106**, 4356.